THE JOURNAL OF PHYSICAL CHEMISTRY A

ARTICLE

pubs.acs.org/JPCA

Acid and Alkali Effects on the Decomposition of HMX Molecule: A Computational Study

Chaoyang Zhang,[†,‡] Yuzhen Li,[†] Ying Xiong,[‡] Xiaolin Wang,[§] and Mingfei Zhou*[,†]

[†]Department of Chemistry, Fudan University, Shanghai 200433, China

[‡]Institute of Chemical Materials, China Academy of Engineering Physics (CAEP), P.O. Box 919-327, Mianyang, Sichuan 621900, China

[§]China Academy of Engineering Physics (CAEP), P.O. Box 919-1, Mianyang, Sichuan 621900, China

ABSTRACT: The stored and wasted explosives are usually in an acid or alkali environment, leading to the importance of exploring the acid and alkali effects on the decomposition mechanism of explosives. The acid and alkali effects on the decomposition of HMX molecule in gaseous state and in aqueous solution at 298 K are studied using quantum chemistry and molecular force field calculations. The results show that both H^+ and OH^- make the decomposition in gaseous state energetically favorable. However, the effect of H^+ is much different from that of OH^- in aqueous solution: OH^- can accelerate the decomposition but H^+ cannot. The difference is mainly caused by the large aqueous solvation energy difference between H^+ and OH^-. The results confirm that the dissociation of HMX is energetically favored only in the base solutions, in good agreement with previous HMX base hydrolysis experimental observations. The different acid and alkali effects on the HMX decomposition are dominated by the large aqueous solvation energy difference between H^+ and OH^-.

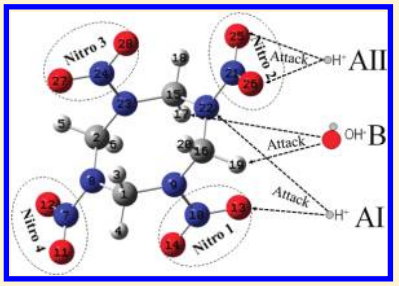

1. INTRODUCTION

It is of great interest to explore the dissociation mechanisms of explosives, attributed to the importance in the security during preparation, storage, transport, use, and waste treatment of explosives. Octahydro-1,3,5,7-tetranitro-1,3,5,7-tetrazocine (HMX) is a well-known energetic material that is extensively applied in explosive and propellant formulations as energetic components.[1] The dissociation mechanism of HMX has been the subject of numerous experimental and theoretical studies.

For a gaseous HMX molecule, it is commonly deemed that there are at least four possible paths for its initial decomposition: $N-NO_2$ bond dissociation, hydrogen transfer and subsequent HONO elimination, C−N bond scission of the ring, and the concerted ring fission. Several results showed that the barriers for the two former paths are close to each other and are much lower than those of the last two paths, suggesting that the two former dissociation paths are energetically favorable. Besides computational investigations on the thermodynamics and kinetics of the above-mentioned decomposition reactions,[2−7] the decomposition mechanism of the excited HMX molecules has been experimentally investigated using various experimental methods such as time-of-flight mass spectrometry and laser-induced fluorescence spectroscopy. It was found that the NO molecule is an initial dissociation product but HONO is not an important intermediate for the excited electronic state decomposition of these cyclic nitramines.[8−10] For condensed HMX, theoretical results showed that the intermolecular hydrogen transfer (to form HONO on an adjacent molecule) is more energetically favorable in δ-HMX than in α-HMX and β-HMX, following the same trend of the HMX sensitivity.[11] A molecular simulation of HMX at a density of 1.9 g/cm^3 and temperature of 3500 K, roughly similar to the condition of the Chapman−Jouget detonation state, has been carried out.[12] The thermal properties of crystal HMX has also been reported.[13]

Besides the structural factors that govern the dissociation mechanism of HMX, some other external factors such as acid−base, metals, and bacteria may also play important roles. The alkali hydrolysis of HMX has been studied by several groups.[14−16] The results showed that HMX can hydrolyze in alkali solution at pH > 10 to form end products including NO_2^-, HCHO, HCOOH, NH_3, and N_2O. Potential intermediates involved in the decomposition paths were proposed. The effect of H^+ and NH_4^+ on the $N-NO_2$ bond dissociation energy of HMX in gaseous state was discussed, leading to the conclusion that acid can accelerate the HMX decomposition in gaseous state.[17] In addition, it was found that HMX decomposition can be accelerated by some metals or metal ions, soil and some bacteria.[18−23]

To have a deep insight into the decomposition mechanism of explosives at different environments, quantum chemistry and molecular force field calculations were performed to study the acid and alkali effects on the decomposition of HMX molecule in gaseous state and in aqueous solution.

2. METHODOLOGIES

As the simplest cases of acid and base, the effects of the H^+ and OH^- ions on dissociation of the HMX molecules in gaseous state and in aqueous solution are accounted here. According to the atomic charges and electrostatic interactions, the attack orientations

Received: May 20, 2011
Revised: August 18, 2011
Published: September 20, 2011

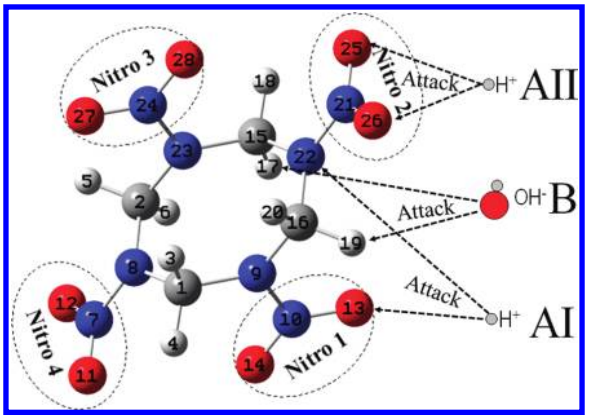

Figure 1. Plot showing the attack orientations of the H^+ and OH^- ions toward the HMX molecule according to the electrostatic interactions.

of H^+ and OH^- to an HMX molecule are proposed as illustrated in Figure 1: the positively charged H^+ can attack the negatively charged oxygen and nitrogen atoms on the molecular ring, and the negatively charged OH^- can attack the positively charged hydrogen atoms. That is, there are two modes (AI and AII) of H^+ attacking an HMX molecule in terms of the location of H^+ relative to the HMX molecule, and only one mode (B) of OH^-. In mode AI, H^+ locates between an oxygen atom like O13 and a neighboring nitrogen atom on the HMX ring like N22. These two atoms are negatively charged and can be attacked by H^+. In mode AII, H^+ locates between the two neighboring oxygen atoms of a nitro group like O25 and O26. Obviously, both negatively charged oxygen atoms can be the attack objects of H^+. In the attack mode of OH^- (B), the positively charged terminal hydrogen atoms of the HMX molecule are the favorite sites for OH^- attack. The ring carbon atoms are difficult to attack due to the steric effect even though they are positively charged. Subsequently, the possible reactions based on these three modes are discussed, including the association of H^+ or OH^- with the HMX molecule, the detachment of a neutral or charged NO_2 fragment and the ring cleavage.

Considering the typical condition of HMX facing up to acid or base, all the calculations were performed at the room temperature (298 K). For gaseous state calculations, the B3LYP/6-311++G(d, p) method[24,25] was employed to fully optimize all the interested structures. The reliability of the optimized structures was verified by frequency analyses: no imaginary frequency for each stable structure and only one obvious imaginary frequency for each transition state (TS) structure. In addition, the thermal energy corrections at 298 K are included in the total energy ($E_{T,298K}$) by frequency calculations.

For aqueous solution calculations, it is assumed that all structures in aqueous solution are the same as those of gaseous state. The possible reactions between these structures and water are not considered here because they belong to subsequent processes. The aqueous solvation effect on these structures was taken into account. Therefore, the total energy of the structures ($E_{T,aq,298K}$) in aqueous solution at 298 K includes their $E_{T,298K}$ and aqueous solvation energies (ΔE_{aq}), as shown in eq 1:

$$E_{T,\,aq,\,298K} = E_{T,\,298K} + \Delta E_{aq,\,298K} \qquad (1)$$

Except for few species including H^+, OH^-, and H_2O whose aqueous solvation energies can be referred,[26] the aqueous solvation energies of other interested species, which are the interaction

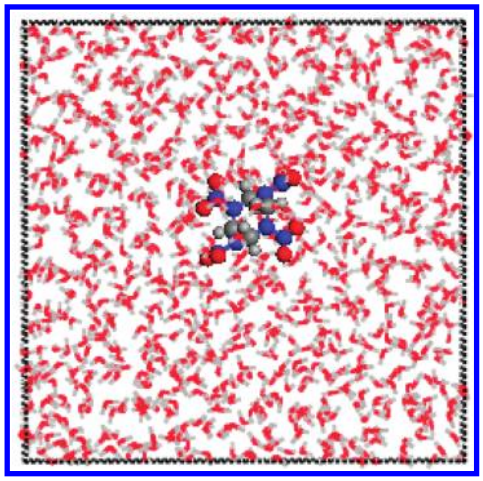

Figure 2. Model for calculating the aqueous solvation energies of the interested species. For example, a HMX molecule is encompassed in water molecules.

energies of these structures with water, were calculated. A combined quantum chemistry and molecular force field method was employed. The detailed process to obtain the aqueous solvation energy follows: (1) Relax the structures of all interested species and water by the BLYP/DNP method[27,28] and assign electrostatic potential (ESP) charges on them. Employ the ESP charges in all force field calculations. (2) Establish a cube with a edge length of 31.04 Å and containing 1000 water molecules with the above assigned ESP charges and a density of 1 g/cm^3, and molecular-dynamically balance the total system using COMPASS force field.[29] (3) Add a molecule of the interested species, for example, an HMX molecule, into the cube and adjust the edge length to make the density of the total system equal to 1 g/cm^3, as illustrated in Figure 2. Molecular-dynamically balance the total system. In all dynamic simulations, the atom based and Ewald summation methods are employed for van de Waals and electrostatic interactions. Each dynamic process lasts for 10 ns with a step of 1 fs. The last process balanced 10 000 steps with 100 step intervals; that is, 100 frames are used to calculate the interaction energy. (4) Obtain the average interaction energy, that is, the average energy difference after the addition of each species into water of the final equilibrium 10 000 steps, and regard it as the aqueous solvation energy of it as shown by eq 2,

$$\Delta E_{aq,\,298K} = \langle E_{int} \rangle = \frac{1}{100} \sum_{i=1}^{100} (E_{T,\,i} - E_{water,\,i} - E_{s,\,i}) \qquad (2)$$

in which $\langle E_{int} \rangle$, $E_{T,i}$, $E_{water,i}$, and $E_{s,i}$ are the average interaction energy between water and the interested species, the total energy of the cube, the energy of the water in the cube removed the interested species, and the energy of the interested species in the cube of ith step, respectively. (5) Adopt the average of the aqueous solvation energies of the two related stable structures as the aqueous solvation energy of a TS structure. All the calculations were carried out using the Gaussian 03[30] and Material Stuido program packages.[31]

The aqueous solvation energies of all involved species are listed in Table 1. For comparison, another kind of aqueous solvation energy of these species are calculated using the PCM method[32] at the B3LYP/6-311++G(d, p) level and the results are also listed in Table 1. The aqueous solvation energies of water,

Table 1. Aqueous Solvation Energies (kcal/mol) of the Species Involved in the Reactions at 298 K

species	$\Delta E_{aq,298K}(C)$	$\Delta E_{aq,,298K}(P)$	$\Delta E_{aq,,298K}(E)^a$	species	$\Delta E_{aq,298K}(C)$	$\Delta E_{aq,298K}(P)$
H^+	−271.4	−102.4	−367.6	AII 1/2	−57.3	−66.8
OH^-	−44.5	−86.3	−43.0	TS2	−57.3	−66.5
H_2O	−11.2	−9.4	−10.5	AII3	−57.4	−59.3
NO_2	−7.5	−1.7		AII4	−59.2	−61.1
NO_2^+	−74.7	−72.0		AII5	−60.1	−62.0
NO_2^-	−62.5	−68.4		B1	−51.5	−47.4
HNO_2	−15.3	−9.4		B2	−49.8	−45.8
HMX	−34.1	−18.7		TS3	−50.6	−46.1
AI1	−53.3	−66.1		B3	−52.9	−48.7
AI2	−57.4	−66.4		B4	−56.7	−53.8
TS1	−55.4	−64.6		B5	−29.8	−14.4
AI3	−22.2	−16.1		B6	−49.5	−49.7
AI4	−52.2	−61.1				

[a] Experimental data cited from ref 26. $\Delta E_{aq,298K}(C)$, $\Delta E_{aq,,298K}(P)$, and $\Delta E_{aq,,298K}(E)$ are calculated aqueous solvation energies using the combined method and PCM method and the experimental aqueous solvation energies, respectively.

Table 2. Bond Lengths (Å) and Bond Orders (in Parentheses) on the Rings of the Species Involved in the Reactions

species	C1−N8	N8−C2	C2−N23	N23−C15	C15−N22	N22−C16	C16−N9	N9−C1
HMX	1.454 (0.96)	1.479 (0.93)	1.443 (0.98)	1.461 (0.95)	1.454 (0.96)	1.479 (0.93)	1.443 (0.98)	1.461 (0.95)
AI1	1.455 (0.96)	1.437 (0.99)	1.494 (0.91)	1.423 (1.02)	1.521 (0.89)	1.514 (0.89)	1.431 (1.01)	1.468 (0.94)
TS1	1.442 (0.99)	1.444 (0.98)	1.486 (0.92)	1.431 (1.00)	1.517 (0.90)	1.484 (0.95)	1.466 (0.95)	1.496 (0.90)
AI2	1.436 (1.00)	1.454 (0.96)	1.473 (0.94)	1.439 (0.99)	1.507 (0.92)	1.463 (0.98)	1.478 (0.92)	1.506 (0.88)
AI3	1.461 (0.95)	1.440 (0.99)	1.485 (0.93)	1.453 (0.96)	1.458 (0.98)	1.438 (1.01)	1.482 (0.92)	1.454 (0.96)
AI4	1.452 (0.96)	1.447 (0.98)	1.479 (0.92)	1.422 (1.03)	1.473 (0.89)	1.461 (0.90)	1.449 (0.99)	1.472 (0.93)
AII 1/2	1.456 (0.96)	1.440 (0.99)	1.487 (0.91)	1.415 (1.03)	1.527 (0.86)	1.520 (0.85)	1.422 (1.02)	1.466 (0.94)
TS2	1.455 (0.96)	1.437 (0.99)	1.492 (0.91)	1.412 (1.04)	1.537 (0.83)	1.530 (0.84)	1.415 (1.04)	1.466 (0.94)
AII3	1.454 (0.98)	1.456 (0.96)	1.469 (0.95)	1.355 (1.04)		1.456 (0.98)	1.454 (0.95)	1.472 (0.92)
AII4	1.467 (0.95)	1.443 (0.99)	1.487 (0.91)	1.412 (1.04)	1.536 (0.85)	1.498 (0.89)	1.438 (1.02)	1.460 (0.98)
AII5	1.464 (0.94)	1.412 (1.04)	1.538 (0.84)	1.467 (0.91)	1.439 (0.98)	1.496 (0.90)	1.434 (1.00)	1.453 (0.96)
B1	1.467 (0.95)	1.477 (0.93)	1.457 (0.96)	1.467 (0.94)	1.469 (0.94)	1.442 (0.98)	1.500 (0.90)	1.445 (0.98)
TS3	1.467 (0.95)	1.480 (0.92)	1.450 (0.98)	1.464 (0.92)	1.462 (0.92)	1.437 (1.00)	1.503 (0.90)	1.446 (0.97)
B2	1.464 (0.95)	1.482 (0.92)	1.446 (0.99)	1.460 (0.90)	1.454 (0.92)	1.433 (1.01)	1.505 (0.89)	1.448 (0.97)
B3	1.457 (0.96)	1.495 (0.90)	1.430 (1.01)	1.430 (0.94)	1.417 (0.93)	1.473 (0.95)	1.447 (0.97)	1.457 (0.96)
B4	1.474 0.96)	1.557 (0.82)	1.399 (1.10)	1.325 (1.31)	1.374 (1.03)	1.466 (0.95)	1.462 (0.95)	1.459 (0.96)
B5	1.476 (0.95)	1.498 (0.92)	1.432 (1.01)	1.267 (1.86)	1.392 (1.04)	1.491 (0.92)	1.454 (0.97)	1.467 (0.95)
B6	1.446 (1.03)		1.367 (1.03)	1.404 (0.99)	1.384 (1.02)	1.468 (0.93)	1.452 (0.98)	1.471 (0.92)

H^+, and OH^- were calculated to be −10.5, +271.4, and −47.3 kcal/mol using the present combined method, which are very close to the experimental data of −11.5, +367.6, and −43.0 kcal/mol.[26] Note that the PCM calculations gave values of −9.4, +102.4, and −86.3 kcal/mol, respectively. Apparently, the present combined method gave much better results than PCM. Thus, only the results calculated with the combined method are used for discussion.

In addition, natural bond orbital (NBO) analyses were performed to determine the molecular stability of all interested species. By thermodynamically analyzing the potential energy surfaces (PES) of each attacking mode, the effects of acid−base on the HMX decomposition under the gaseous and the aqueous solution conditions were determined. It should be noted that only the initial steps of HMX decomposition were calculated and the subsequent steps to finial small molecule products or the reactions with water were not considered.

3. RESULTS AND DISCUSSION

We will focus on changes of strength of the bonds on the ring and the N−N bonds and the charges of the nitro groups and hydrogen atoms upon H^+ or OH^- attacking, in that they are the most possible active points in the initial decomposition processes. The results are summarized in Tables 2−4. We will discuss the effects of acid−base on the decomposition of HMX molecules according to the three modes: AI, AII, and B.

3.1. Mode AI. The related structures belonging to mode AI are indicated in Figure 3. In this mode, H^+ attacks either an oxygen atom or a nitrogen atom on the ring to form AI1 or AI2. There is a transition state structure, TS1, between AI1 and AI2. As AI2 is similar to AII1, which will be discussed in the next section, we only pay attention to the decomposition of AI1 in this section. As shown in Figure 3, the newly formed N22−H29 bond in AI1 has a bond length of 1.029 Å with the bond order of 0.90.

Table 3. Bond Lengths (Å), Bond Orders (in Parentheses), and Charges on Nitro Groups (e, in Brackets) of the Species Involved in the Reactions

species	nitro 1 (N9−N10)	Nitro 2 (N21−N22)	nitro 3 (N23−N24)	nitro 4 (N7−N8)
HMX	1.401 (0.93) [−0.085]	1.391 (0.94) [−0.093]	1.401 (0.93) [−0.085]	1.391 (0.94) [−0.093]
AI1	1.429 (0.89) [−0.028]	1.792 (0.50) [0.361]	1.404 (0.92) [−0.059]	1.431 (0.89) [−0.047]
TS1	1.369 (1.00) [0.179]	1.588 (0.73) [0.106]	1.409 (0.91) [−0.053]	1.439 (0.88) [−0.039]
AI2	1.336 (1.07) [0.297]	1.517 (0.81) [0.015]	1.412 (0.91) [−0.054]	1.435 (0.88) [−0.048]
AI3	1.392 (0.94) [−0.107]		1.380(0.96) [−0.115]	1.410 (0.91) [−0.077]
AI4	1.460 (0.85) [−0.001]		1.423 (0.89) [−0.026]	1.425 (0.89) [−0.058]
AII 1/2	1.440(0.87) [−0.028]	1.297 (1.20) [−0.056]	1.419 (0.90) [−0.044]	1.426 (0.89) [−0.056]
TS2	1.446 (0.87) [−0.016]	1.273 (1.33) [0.076]	1.420 (0.90) [−0.041]	1.429 (0.89) [−0.049]
AII3	1.360 (1.00) [0.206]	1.296 (1.28) [0.122]	1.386 (0.97) [−0.114]	1.420 (0.90) [−0.067]
AII4		1.294 (1.20) [0.207]	1.425 (0.89) [−0.039]	1.439 (0.88) [−0.049]
AII5	1.444 (0.87) [−0.025]		1.813 (0.46) [0.350]	1.451 (0.86) [−0.008]
B1	1.371 (0.98) [−0.150]	1.387 (0.95) [−0.148]	1.382 (0.96) [−0.154]	1.384 (0.97) [−0.139]
TS3	1.368 (0.98) [−0.153]	1.400 (0.94) [−0.176]	1.387 (0.96) [−0.185]	1.381 (0.96) [−0.136]
B2	1.366 (0.99) [−0.160]	1.417 (0.92) [−0.198]	1.395 (0.96) [−0.208]	1.378 (0.97) [−0.140]
B3	1.382 (0.96) [−0.125]	1.365 (1.02) [−0.267]	1.419 (0.91) [−0.248]	1.372 (0.99) [−0.164]
B4	1.385 (0.96) [−0.140]	1.386 (1.01) [−0.407]		1.378 (0.99) [−0.208]
B5	1.402 (0.93) [−0.094]	1.415 (0.91) [−0.061]		1.393 (0.94) [−0.106]
B6	1.390 (0.96) [−0.148]	1.422 (0.90) [−0.100]	1.411 (0.95) [−0.164]	1.311 (1.22) [−0.473]

Table 4. Charges on the Hydrogen Atoms (e) of the Species Involved in the Reactions

species	H3	H4	H5	H6	H17	H18	H19	H20
HMX	0.064	0.098	0.087	0.064	0.064	0.098	0.087	0.064
AI1	0.083	0.121	0.095	0.102	0.101	0.106	0.104	0.094
TS1	0.099	0.115	0.096	0.103	0.080	0.116	0.111	0.097
AI2	0.103	0.111	0.101	0.101	0.072	0.113	0.113	0.091
AI3	0.062	0.109	0.062	0.084	0.039	0.077	0.069	0.048
AI4	0.085	0.120	0.106	0.105	0.127	0.142	0.132	0.111
AII 1/2	0.081	0.118	0.098	0.010	0.099	0.103	0.113	0.096
TS2	0.082	0.120	0.097	0.101	0.106	0.111	0.114	0.099
AII3	0.094	0.096	0.082	0.093	0.057	0.066	0.091	0.142
AII4	0.067	0.103	0.099	0.098	0.103	0.105	0.108	0.080
AII5	0.082	0.129	0.093	0.122	0.095	0.112	0.124	0.089
B1	0.050	0.092	0.067	0.144	0.145	0.074	0.146	0.054
TS3	0.059	0.089	0.073	0.100	0.198	0.012	0.106	0.059
B2	0.063	0.088	0.073	0.073	0.223	−0.022	0.078	0.059
B3	0.065	0.079	0.049	0.064		−0.038	0.068	0.040
B4	0.057	0.072	0.002	0.007		−0.006	0.081	0.060
B5	0.066	0.096	0.056	0.053		0.059	0.095	0.076
B6	0.016	0.039	0.039	0.090		0.053	0.083	0.058

The positive charge of H^+ is apparently transferred upon combination to the nitrogen atom, with only 0.260 e remaining. In contrast to the HMX molecule, the molecular stability of AI1 decreases significantly as the N22−N21 bond is elongated from 1.454 to 1.792 Å with its bond order reduced from 0.94 to 0.50. The charge on the nitro 2 subunit changes from negative (−0.093 e) to positive (+0.361 e), as shown in Table 3. The positively charged nitro group implies its easy detachment.[33] The weak bond of N22−N21 suggests an obvious potential trigger linkage of AI1. As indicated in Table 2, the other two bonds of the N22 atom, C15−N22 and C16−N22, are also weakened with their bond lengths elongated from 1.454 and 1.479 Å to 1.521 and 1.514 Å, respectively. Summarily, after combining H^+ to the nitrogen atom of the HMX ring, a new less stable AI1 is formed in which all the three bonds linking with the nitrogen atom are weakened.

The N22−N21 bond in AI1 is the weakest, implying that this bond is the easiest one for rupture. Two styles of nitro 2 elimination are considered: formation of AI4 with the removal of a neutral nitro group and formation of AI3 with the elimination of a positively charged nitro group, as shown in Figure 3. After removal of the neutral or positively charged nitro 2 group, the AI4 or AI3 residuals are stabilized relative to AI1. This can be deduced from the structural parameters of AI3 and AI4 shown in Tables 2 and 3. The C−N bonds on the ring are averaged after the removal of the nitro group with the bond length range changes from 1.423 to 1.521 Å in AI1 to 1.438−1.485 Å in AI3 and to 1.422−1.473 Å in AI4. All the N−N bonds in AI3 and AI4 are much shorter than 1.792 Å, suggesting that they are stronger than the N21−N22 bond in AI1.

The potential energy profiles of the reactions based on mode AI are shown in Figure 4. The association reactions between HMX and H^+ in gaseous state in forming AI1 or AI2 were predicted to be highly exothermic (over 174 kcal/mol at 298 K). There is a small energy barrier connecting AI1 and AI2, suggesting easy conversion between AI1 and AI2. The association reaction energy is sufficient to overcome the barriers of subsequent decomposition reactions of AI1 to AI4 + NO_2 or AI3 + NO_2^+, both of which were predicted to be endothermic. In contrast, the association reaction between HMX and H^+ in aqueous solution is highly endothermic with more than 68 kcal/mol heat required, far above the bond dissociation energy of N−NO_2 in HMX (37 kcal/mol).[34] This indicates that there is no effect of H^+ on the decomposition. The dissociation reactions of AI1 to AI4 + NO_2 and AI3 + NO_2^+ in aqueous solution are exothermic, which are different from those in gaseous state. These results clearly indicate that there is large thermodynamic difference of

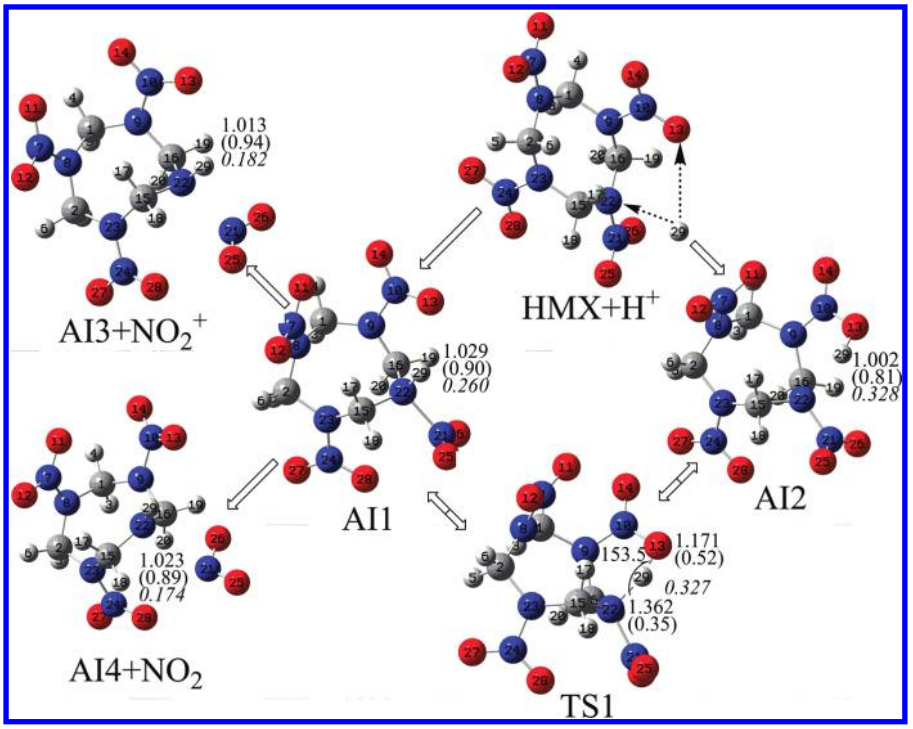

Figure 3. Species related to the AI mode. Bond length (Å), bond order in parentheses, and bond angle and atomic charges in italic type of attacking hydrogen atom (numbered as 29) are indicated.

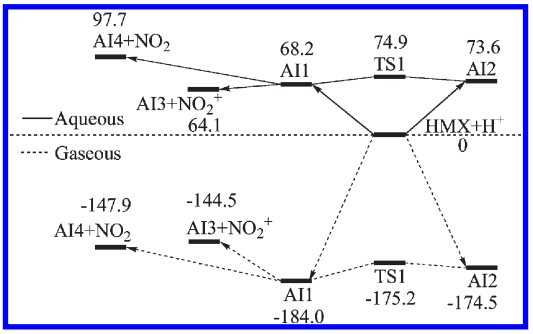

Figure 4. Potential energy profiles (values in kcal/mol) of the reactions at 298 K based on the AI mode.

the effect of acid on the HMX decomposition in gaseous state and in aqueous solution, due to the large aqueous solvation energy of H^+, the calculated value of 271.4 kcal/mol or experimental value of 367.7 kcal/mol. Previous study showed that the acid can accelerate the HMX decomposition based only on gaseous state calculations, suggesting that the mixing of HMX and acid should be avoided.[17] The present calculation results clearly show that acid can accelerate the HMX decomposition in gaseous state but cannot in aqueous solution. Thus, it is unnecessary to avoid mixing of HMX and acid in aqueous solution.

3.2. Mode AII. The reactions of mode AII are illustrated in Figure 5. H^+ interacts with one of oxygen atoms of a nitro group of HMX to form AII1 or AII2, which have similar structures and are interconvertible through a transition state TS2. Thus, only the structure and reactions of AII1 are discussed. Note that AII2 is a structural conformer of AI2 by the rotation of the O−H bond.

Upon H^+ association to the HMX molecule in forming AII2, the C−N bond lengths of the molecular ring change significantly. As listed in Table 2, some bonds are strengthened whereas others are weakened. The difference between the maximum and the minimum bond length increases from 0.036 Å (1.479−1.443) in AMX to 0.112 Å (1.527−1.415) in AII2. The C15−N22 and N22−C16 bonds have the longest bond lengths of 1.527 and 1.520 Å, which implies that these two bonds are the most possible triggers of the ring cleavage. For the N−N bonds, only the N21−N22 bond is shortened whereas the others are elongated. The N9−N10 bond has the longest bond length of 1.440 Å, suggesting that it is the easiest one for rupture. Accordingly, the possible dissociation reactions of AII1 are either ring-opening in forming AII3 or NO_2 elimination with the formation of AII4 + NO_2. In addition, the detachment of an NOOH fragment followed by hydrogen atom transfer in producing AII5 + NOOH is also considered,[6] as illustrated in Figure 5. The structural parameters of AII3, AII4, and AII5 are listed in Tables 2 and 3. With respect to the HMX molecule, the bond lengths of AII3 are only slightly changed, whereas all the N−N bonds of AII5 are obviously lengthened. The C15−N22 bond is elongated from 1.454 Å in HMX to 1.536 Å in AII4, implying that this bond is the potential trigger of further dissociation of AII4.

The potential energy profiles of the reactions based on mode AII are shown in Figure 6. The formation of AII5 + NOOH is the most favorable reaction channel in both gaseous state and aqueous solution. Similar to mode AI, the association reactions between HMX and H^+ in gaseous state in forming AII1 or AII2 were predicted to be highly exothermic. Although the subsequent reactions from AII1 to AII3, AII4, and AII5 are all endothermic, the overall reactions from HMX + H^+ to AII3, AII4, and AII5 are exothermic, suggesting that these reactions are energetically favorable in gaseous state. In contrast, these reactions are highly

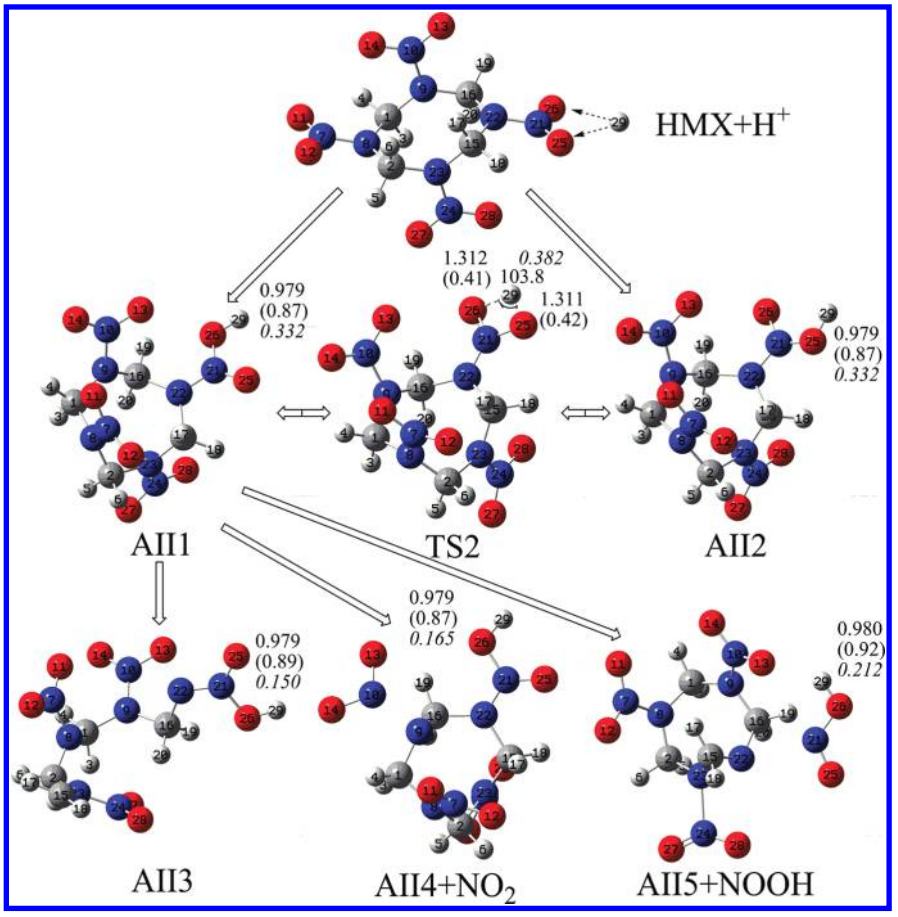

Figure 5. Species related to the AII mode. Bond length (Å), bond order in parentheses, and bond angle and atomic charges in italic type of attacking hydrogen atom (numbered as 29) are indicated.

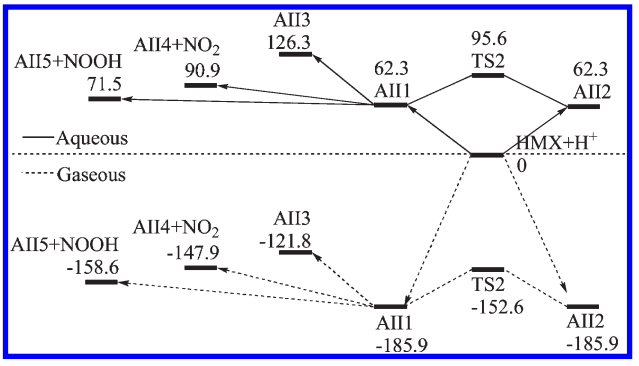

Figure 6. Potential energy profiles (values in kcal/mol) of the reactions at 298 K based on the AII mode.

endothermic in aqueous solution, indicating that there is no effect of H^+ on the decomposition of HMX.

The potential energy profiles shown in Figures 4 and 6 clearly demonstrate that the acid under gaseous condition can strongly accelerate the HMX molecule decomposition, but the acid in aqueous solution has no effect on the HMX molecule decomposition. Such a large difference is assumed to be caused by the big aqueous solvation energy of H^+.

3.3. Mode of B. The reactions of mode B are shown in Figure 7. The effect of base, OH^-, on the decomposition of the HMX molecule is realized by the initial association of the HMX molecule and OH^- in forming a complex B1, in which OH^- is feebly coordinated to the HMX molecule through three neighboring hydrogen atoms with O---H distances of 1.857, 1.857, and 1.823 Å, respectively. From B1, the OH^- fragment takes a proton from HMX in forming B2 via a transition state TS3. The B2 intermediate is a water complex, which can be transferred to B3 with the removal of a water molecule. B3 can be regarded as an anion formed via removing a proton from the HMX molecule.

Compared to the HMX molecule, B3 has two triggers possibly, leading to its decomposition, namely the weakened N8—C2 and N23—N24 bonds. The N8—C2 bond broken results in the ring-opening with the formation of product B6, whereas the N23—N24 bond dissociation leads to the production of B4 and NO_2 fragments. Because the negative charge of B3 is mainly located on the nitro groups, the channel for the formation of B5 and NO_2^- is also considered. Relative to B3, the N8—C2 bond in B4 is significantly weakened, whereas its C2—N23, N23—C15, and C15—N22 bonds are strengthened. In B5, the N23—C15 bond is shortened to be a formal double bond with a bond order of 1.86. In B6, the C1—N8 and C2—N23 bonds are strengthened, whereas the other bonds are only slightly changed.

The potential energy profiles of the reactions based on mode B are shown in Figure 8. Different from the reactions of mode AI and AII, all the reaction intermediates and products involved in mode B are lower in energy than the reactants: HMX + OH^- in both gaseous state and aqueous solution, suggesting that these reactions are energetically favored. And all reactions in gaseous

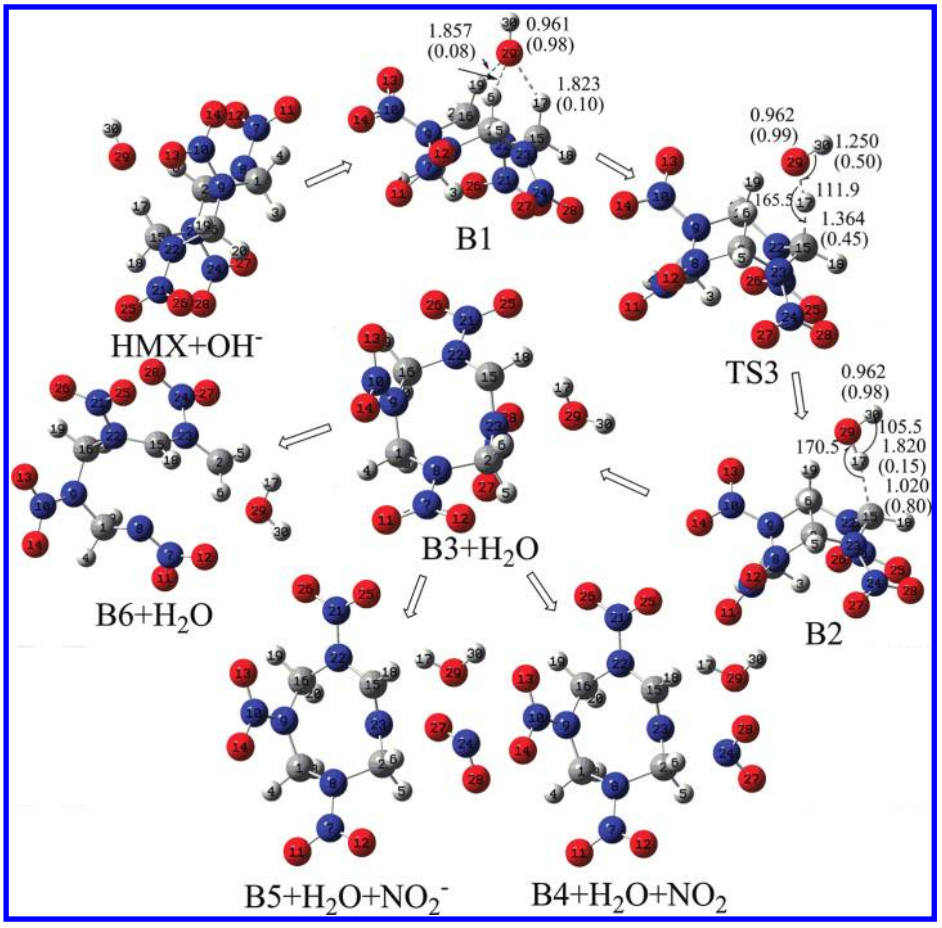

Figure 7. Species related to the B mode. Bond length (Å), bond order in parentheses, and bond angle of attcking OH^- (numbered as 29 and 30 for the oxygen and hydrogen atoms, respectively) are indicated.

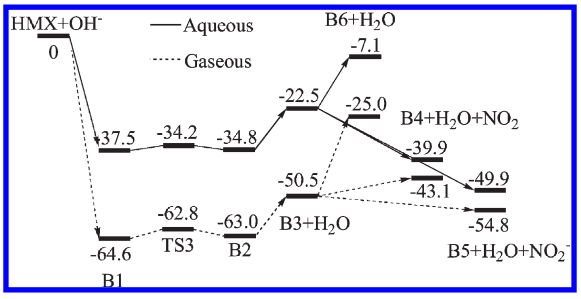

Figure 8. Potential energy profiles (values in kcal/mol) of the reactions at 298 K based on the B mode.

state seem to be correspondingly easier than those in aqueous solution. The formation of B5 + NO_2^- is the most energetically favored reaction channel in both gaseous state and aqueous solution. Of more importance, the reactions leading to the formation of B4 and B5 are more energetically favored than B6 in aqueous solution, which is consistent with previous HMX hydrolysis experimental observations.[14−16]

4. CONCLUSIONS

The effects of acid and base on the decomposition of HMX in gaseous state and in aqueous solution were investigated using quantum chemistry and molecular force field calculations. The results show that both H^+ and OH^- make the decomposition in gaseous state energetically favorable. However, the effect of H^+ is much different from that of OH^- in aqueous solution: OH^- can accelerate the decomposition but H^+ cannot. The difference is caused by the difference of the aqueous solvation energies of the related species, in particular, the large aqueous solvation energy difference between H^+ and OH^-. The results confirm that the dissociation of HMX is energetically favored only in the base solutions, in good agreement with previous HMX base hydrolysis experimental observations.

AUTHOR INFORMATION

Corresponding Author

*E-mail: mfzhou@fudan.edu.cn.

ACKNOWLEDGMENT

Financial support from the CAEP's fund (2011A0302014), the State Key Development Program for Basic Research of China (973-61383), and the National Natural Science Foundation of China (Nos 21173199 and 10972025) is greatly appreciated.

REFERENCES

(1) Dong, H.; Zhou, F. *Properties of High Explosives and Their Relatives*; Science Press: Beijing, 1989.

(2) Zhang, S.; Truong, T. *J. Phys. Chem. A* **2000**, *104*, 7304.
(3) Zhang, S.; Truong, T. *J. Phys. Chem. A* **2001**, *105*, 2427.
(4) Zhang, S.; Nguyen, H.; Truong, T. *J. Phys. Chem. A* **2003**, *107*, 2981.
(5) Chakraborty, D.; Muller, R.; Dasgupta, S.; Goddard, W. *J. Phys. Chem. A* **2001**, *105*, 1302.
(6) Lewis, J.; Glaesemann, K.; VanOpdorp, K.; Voth, G. *J. Phys. Chem. A* **2000**, *104*, 11384.
(7) Lyman, J.; Liau, Y.; Brand, H. *Combust. Flame* **2002**, *130*, 185.
(8) Guo, Y.; Greenfield, M.; Bernstein, E. *J. Chem. Phys.* **2005**, *122*, 244310.
(9) Greenfield, M.; Guo, Y.; Bernstein, E. *Chem. Phys. Lett.* **2006**, *430*, 277.
(10) Guo, Y.; Greenfield, M.; Bhattacharya, A.; Bernstein, E. *J. Chem. Phys.* **2007**, *127*, 154301.
(11) Lewis, J. *Chem. Phys. Lett.* **2003**, *371*, 588.
(12) Manaa, M.; Fried, L.; Melius, C.; Elstner, M.; Frauenheim, T. *J. Phys. Chem. A* **2002**, *106*, 9024.
(13) Hobbs, M. *Thermochim. Acta* **2002**, *384*, 291.
(14) Balakrishnan, V.; Halasz, A.; Hawari, J. *Environ. Sci. Technol.* **2003**, *37*, 1838.
(15) Bishop, R.; Flesner, R.; Dell'Orco, P.; Spontarelli, T.; Larson, S. *Ind. Eng. Chem. Res.* **1999**, *38*, 2254.
(16) Heilmann, H.; Wiesmann, U.; Stenstrom, M. *Environ. Sci. Technol.* **1996**, *30*, 1485.
(17) Wang, L.; Lin, Y.; Tuo, X. *Acta Phys.-Chin. Sin.* **2007**, *23*, 1560.
(18) Monteil-Rivera, F.; Paquet, L.; Halasz, A.; Montgomery, M.; Hawari, J. *Environ. Sci. Technol.* **2005**, *39*, 9725.
(19) Fournier, D.; Halasz, A.; Thiboutot, S.; Ampleman, G.; Manno, D.; Hawari, J. *Environ. Sci. Technol.* **2004**, *38*, 4130.
(20) Hawari, J.; Halasz, A.; Beaudet, S.; Paquet, L.; Ampleman, G.; Thiboutot, S. *Environ. Sci. Technol.* **2001**, *35*, 70.
(21) Bhushan, B.; Halasz, A.; Thiboutot, S.; Ampleman, G.; Hawaria, J. *Biochem. Biophys. Res. Commun.* **2004**, *316*, 816.
(22) Zoha, Kyung-Duk; Stenstrom, Michael K. *Water Res.* **2002**, *36*, 1331.
(23) Monteil-Rivera, F.; Groom, C.; Hawari, J. *Environ. Sci. Technol.* **2003**, *37*, 3878.
(24) Becke, A. D. *J. Chem. Phys.* **1993**, *98*, 5648.
(25) Lee, C.; Yang, W.; Parr, R. G. *Phys. Rev. B* **1988**, *37*, 785.
(26) Cao, X.; Song, T.; Wang, X. *Organic Chemistry*, 3rd ed.; High Education Press: Beijing, 1994.
(27) Delley, B. *J. Chem. Phys.* **1990**, *92*, 508.
(28) Delley, B. *J. Chem. Phys.* **2000**, *113*, 7756.
(29) Sun, H. *J. Phys. Chem. B.* **1998**, *102*, 7338.
(30) Frisch, M. J.; Trucks, G. W.; Schlegel, H. B.; Scuseria, G. E.; Robb, M. A.; Cheeseman, J. R.; Montgomery, J. A., Jr.; Vreven, T.; Kudin, K. N.; Burant, J. C.; Millam, J. M.; Iyengar, S. S.; Tomasi, J.; Barone, V.; Mennucci, B.; Cossi, M.; Scalmani, G.; Rega, N.; Petersson, G. A.; Nakatsuji, H.; Hada, M.; Ehara, M.; Toyota, K.; Fukuda, R.; Hasegawa, J.; Ishida, M.; Nakajima, T.; Honda, Y.; Kitao, O.; Nakai, H.; Klene, M.; Li, X.; Knox, J. E.; Hratchian, H. P.; Cross, J. B.; Adamo, C.; Jaramillo, J.; Gomperts, R.; Stratmann, R. E.; Yazyev, O.; Austin, A. J.; Cammi, R.; Pomelli, C.; Ochterski, J. W.; Ayala, P. Y.; Morokuma, K.; Voth, G. A.; Salvador, P.; Dannenberg, J. J.; Zakrzewski, V. G.; Dapprich, S.; Daniels, A. D.; Strain, M. C.; Farkas, O.; Malick, D. K.; Rabuck, A. D.; Raghavachari, K.; Foresman, J. B.; Ortiz, J. V.; Cui, Q.; Baboul, A. G.; Clifford, S.; Cioslowski, J.; Stefanov, B. B.; Liu, G.; Liashenko, A.; Piskorz, P.; Komaromi, I.; Martin, R. L.; Fox, D. J.; Keith, T.; Al-Laham, M. A.; Peng, C. Y.; Nanayakkara, A.; Challacombe, M.; Gill, P. M. W.; Johnson, B.; Chen, W.; Wong, M. W.; Gonzalez, C.; Pople, J. A. *Gaussian 03*, Revision B.05; Gaussian, Inc.: Pittsburgh, PA, 2003.
(31) *Material Studio 4.0*; Acceryls Inc.: San Diego, 2005.
(32) Eckert, F.; Klamt, A. *AIChE J.* **2002**, *48*, 369.
(33) Zhang, C.; Shu, Y.; Huang, Y.; Zhao, X.; Dong, H. *J. Phys. Chem. B* **2005**, *109*, 8978.
(34) Calculated at the B3LYP/6-311++G** level.